

# Chapter 2

## Literature overview

### **2.1 Parkinson's disease**

#### **2.1.1 General background**

PD was first described in 1817 by James Parkinson and is today the second most common age-related neurodegenerative disorder after Alzheimer's disease (AD) (Dauer & Przedborski, 2003). Age is the main risk factor for developing PD. PD is observed in 17.4 out of 100 000 people between the ages of 50 and 59 and in 93.1 out of 100 000 people between the ages of 70 and 79 (Lees *et al.*, 2009).

Parkinsonism and PD are commonly seen as the same disorder but it differs significantly. Bradykinesia (slowness of movement), muscular rigidity, resting tremor and freezing are symptoms of parkinsonism as well as PD (Lang & Lozano, 1998). In contrast to parkinsonism, PD is a degenerative disease where there is a loss of dopaminergic neurons in the SNpc. In contrast, various forms of DA deficiency or striatal damage may lead to parkinsonism. PD, otherwise known as idiopathic PD, can thus be seen as a syndrome whereas parkinsonism can be caused by factors other than age-related degeneration of neurons such as drugs (anti-psycotics and DA antagonists), hypoxia, trauma and tumors (Dauer & Przedborski, 2003). Other characteristics and symptoms of PD include depression, dementia, sleep problems, speech difficulty, hallucinations and bladder problems (Tugwell, 2008). It is difficult to identify the precise mode of death of the PD patient, but pneumonia is the most common cause (Lees *et al.*, 2009).

#### **2.1.2 Pathophysiology**

The SNpc, via the nigrostriatal pathway, provides dopaminergic innervations to the putamen in the basal ganglia (Standaert & Young, 2006). As mentioned earlier, PD is a degenerative disorder where there is a loss of DA neurons in the SNpc which leads to a dramatic decrease of DA in the basal ganglia and depigmentation of the SNpc (figure 2.1) (Dauer & Przedborski, 2003). The functional loss of DA from the striatum is directly responsible for the motor symptoms of PD. This led to the conclusion that replacement of DA function could be a strategy for the treatment of PD (Cotzias *et al.*, 1969; Hornykiewicz, 1973).

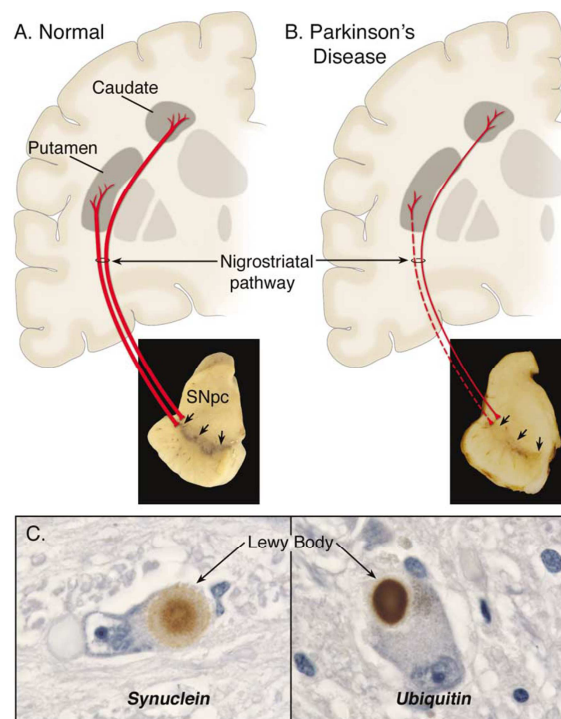


**Figure 2.1.** Pathophysiology of PD (**A**), showing in red, the normal nigrostriatal pathway, containing dopaminergic neurons, whose cell bodies are located in the SNpc, (**B**) illustrating the degenerating nigrostriatal pathway and depigmentation of the SNpc and (**C**) the immunohistochemical labeling of intraneuronal inclusions named Lewy bodies (Dauer & Przedborski, 2003).

### 2.1.3 The role of dopamine in Parkinson's disease

DA plays a major role in the neurochemistry of PD. DA is a catecholamine and is synthesized from tyrosine in the terminals of dopaminergic neurons (Youdim *et al.*, 2006). The synthesis and metabolism of DA are summarized in figure 2.2. As shown in figure 2.2, DA is metabolized by MAO-A and MAO-B and catechol-O-methyl transferase (COMT). DA is metabolized by MAO to ultimately form 3,4-dihydroxyphenylacetic acid (DOPAC). The MAO catalytic cycle generates the potentially toxic compound, hydrogen peroxide, which may subsequently be converted to oxyradicals. Left unchecked, these reactive species can lead to DNA damage, peroxidation of membrane lipids and neuronal death. Ferrous iron, which is relatively abundant in the basal ganglia, can generate hydroxyl free radicals in the presence of hydrogen peroxide and if the protective mechanisms are inadequate, because of inherited or acquired deficiency, the oxyradicals could cause the degeneration of dopaminergic neurons. This is termed the Fenton reaction (Standaert & Young, 2006).

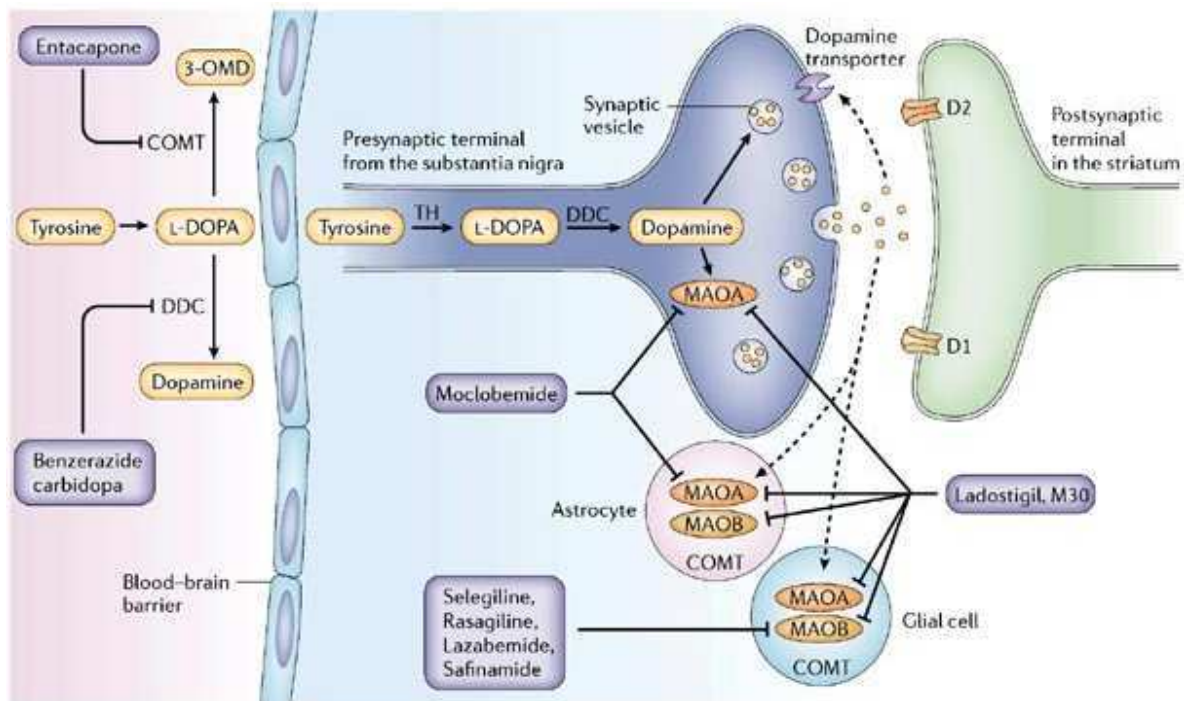


**Figure 2.2.** DA synthesis and metabolism by MAO-A and MAO-B (Youdim *et al.*, 2006).

### 2.1.4 Aetiology

The cause of PD is unknown, and it is therefore still unclear as to how much of the disease results from a purely environmental factor, a genetic causation or a combination of both (Di Monte, 2003; Steece-Collier *et al.*, 2002). Environmental agents, such as paraquat (a herbicide) and rotenone (garden insecticide/fish toxin) have been shown to induce dopaminergic cell degeneration (figure 2.3) (Betarbet *et al.*, 2000; Brooks *et al.*, 1999; Chun *et al.*, 2001), but convincing evidence of the role of such compounds in PD is still lacking (Tugwell, 2008).

A number of genes have been identified that may be linked to PD as shown in table 2.1. One of these is the gene encoding the protein,  $\alpha$ -synuclein. Lewy bodies which are formed in PD, contain oxidatively modified  $\alpha$ -synuclein, which *in vitro* exhibits a greater tendency to aggregate than unmodified  $\alpha$ -synuclein (Giasson *et al.*, 2000). Aggregated or soluble misfolded protein could be neurotoxic through a variety of mechanisms. Interference with intracellular trafficking in neurons or deforming the cell itself are the direct damages that could be caused by protein aggregates (Dauer & Przedborski, 2003).

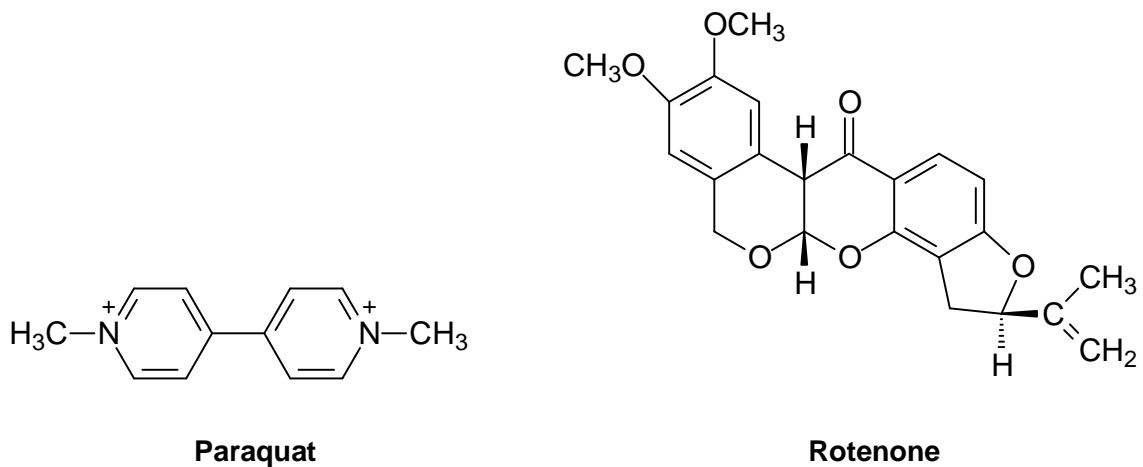


**Figure 2.3.** Chemical structures of paraquat and rotenone.

Another gene that might be involved in PD is LRRK-2, a kinase encoding the protein dardarin. The most common mutation is the Gly2019Ser mutation which has a frequency of 1% in sporadic cases, and 4% in patients with hereditary parkinsonism (Paisán-Ruíz *et al.*, 2004; Healy *et al.*, 2008). Studies have shown that almost a third of North African Arabs, which has been diagnosed with PD, has a LRRK-2 mutation. This mutation is also common in Ashkenazi Jews and Portuguese people. When the Gly2019Ser mutation is inherited, people under the age of 60 have a 28% chance in developing PD whereas people 79 years of age have a 74% probability (Healy *et al.*, 2008).

**Table 2.1.** Genes that are involved in inherited PD

- |  |
|--|
| <ul style="list-style-type: none"> <li>• <math>\alpha</math>-Synuclein (PARK1)</li> <li>• Parkin (PARK2)</li> <li>• Ubiquitin carboxy terminal hydrolase-L1 (UCHL1)</li> <li>• DJ-1 (PARK7)</li> <li>• Nuclear receptor subfamily 4, group A, member 2 (NR4A2)</li> <li>• Leucine rich repeat kinase 2 (LRRK-2)</li> </ul> |
|--|

### 2.1.5 Treatment

Various treatment options are available for PD, including DA receptor agonists (pramipexole and ropinirole), L-Dopa in combination with a DA decarboxylase inhibitor such as benserazide (which should always be used as initial treatment), COMT inhibitors (tolcapone and entacapone), anticholinergic drugs (orphenadrine and benztropine), adenosine  $A_{2A}$  receptor antagonists (KW 6002), anti-viral preparations (amantadine) and MAO-B inhibitors (selegiline and rasagiline) (Standaert & Young, 2006).

L-Dopa is a DA precursor, and undergoes decarboxylation in both the periphery and central nervous system (CNS) to form DA. L-Dopa is rapidly metabolized by COMT to form 3-O-methyldopa. L-Dopa is also decarboxylated by aromatic L-amino acid decarboxylase to yield DA. Since DA does not cross the blood-brain barrier (BBB), a peripheral acting decarboxylase inhibitor such as carbidopa or benserazide is administered with L-Dopa. These drugs prevent the peripheral decarboxylation of L-Dopa. L-Dopa, which crosses the BBB, is preferentially decarboxylated in the CNS to form DA, where it then can bind to DA receptors to provide the desired effect (Standaert & Young, 2006).

DA receptor agonists, unlike L-Dopa, do not require enzymatic conversion to an active metabolite, have no potential toxic effects and do not compete with other substances for active transport across the BBB. Ropinirole and pramipexole have selective activity at  $D_2$  receptor sites and little or no activity at  $D_1$  receptor sites. They are very well absorbed and have a longer duration of action compared to L-Dopa. DA agonists are particularly effective in patients who have developed the on/off phenomena (Standaert & Young, 2006).

As mentioned, COMT is responsible for the catabolism of levodopa to form the inactive compound 3-O-methyldopa, both in the periphery and in the CNS. DA is also metabolized by COMT to form 3-methoxytyramine. COMT inhibitors, such as tolcapone and entacapone, are thus administered to increase levels of L-Dopa peripherally and to decrease DA breakdown in the CNS (Standaert & Young, 2006).

Amantadine, which was originally used as an antiviral agent, was by chance found to have antiparkinsonian properties. Its mode of action is unclear, but it may potentiate dopaminergic function by influencing the synthesis, release and reuptake of DA in the CNS (Standaert & Young, 2006).

Anticholinergic drugs were used widely for the treatment of PD before the discovery of L-Dopa. Anticholinergic drugs do not increase the levels of DA but rather only decrease involuntary movements associated with PD by restoring the balance between the dopaminergic and cholinergic systems in the CNS. In PD, the degeneration of the dopaminergic neurons is thought to result in an overactivity of the cholinergic system (Standaert & Young, 2006).

MAO-B inhibitors, another class of drugs used in PD therapy, are discussed in section 2.2.6.

## **2.2 Monoamine oxidase**

### **2.2.1 General background**

The MAOs are mitochondrial outer membrane bound flavoproteins that catalyze the oxidative deamination of neurotransmitters and biogenic amines (Edmondson *et al.*, 2004). These substrates include monoamines such as 5-HT, histamine and the catecholamines, DA, noradrenaline (NA) and adrenaline (Youdim *et al.*, 1988; Shih *et al.*, 1999; Tipton *et al.*, 2004).

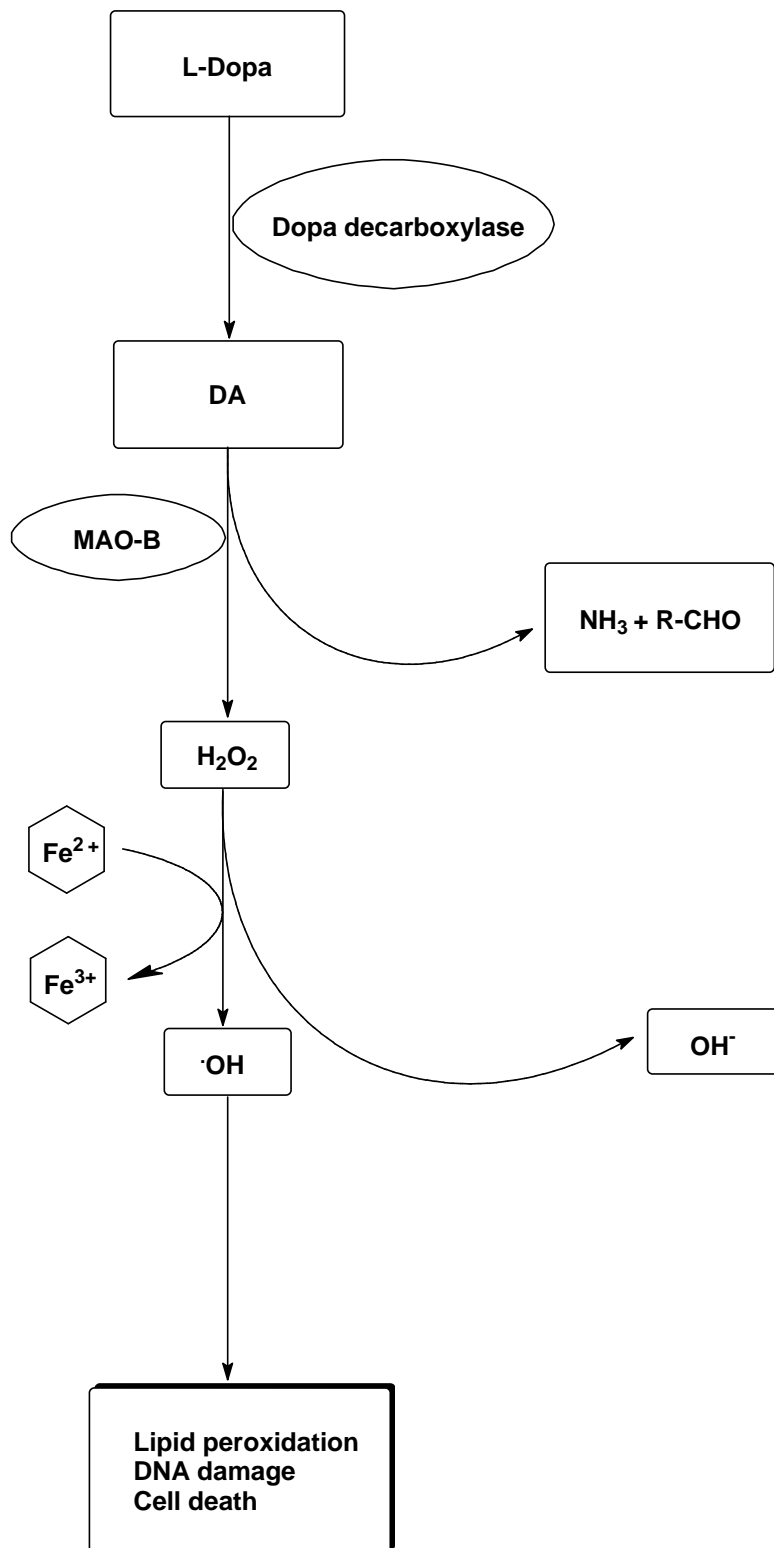
MAO inhibitors were among the first antidepressants to be discovered. Some of these inhibitors were also shown to have potential uses in the treatment of several neurodegenerative conditions, including PD and AD (Youdim *et al.*, 2006). Investigations have found that there are two isoforms of MAO, namely MAO-A and MAO-B. MAO-A inhibitors are used as antidepressants whereas MAO-B inhibitors have a therapeutic role in the treatment of PD (Youdim & Bakhle, 2006). As mentioned, the MAOs have a variety of substrates and the substrate specificities of MAO-A and MAO-B differ. MAO-A shows preference for the metabolism of NA and 5-HT whereas MAO-B preferentially metabolizes benzylamine (Johnston, 1968). To show this, MAO-A deficient mice were produced, using gene knockout techniques (Cases *et al.*, 1995). In this case, the 5-HT concentrations were increased up to nine-fold in mouse pups when compared to normal, wild-type mice pups. The concentrations of 5-HT was only increased two-fold in adult mice brains because of the increased MAO-B levels (Lenders *et al.*, 1996). This led to the conclusion that, when MAO-A is not functioning, MAO-B may take over and oxidize those substrates that are usually oxidized by MAO-A (Berry *et al.*, 1994a; Berry *et al.*, 1994b). Both isoforms metabolize DA and tyramine (Youdim *et al.*, 2005).

MAO is present in most mammalian tissues, but the proportions of the two isoenzymes vary from tissue to tissue (Youdim *et al.*, 1988). MAO-A consists of 527 amino acids whilst MAO-B consists of 520 amino acids and the two isoforms have a 70% sequence identity at the amino acid level (Kearney *et al.*, 1971). Both isoforms are 60-kDa proteins (Shih *et al.*, 1999).

### 2.2.2 The role of MAO in Parkinson's disease

The two isoenzymes of MAO are not evenly distributed in the brain, and the main form in the basal ganglia is MAO-B. As mentioned earlier, the SNpc provides dopaminergic innervations to the basal ganglia, and since MAO-B is the predominant isoform in that area, DA oxidation in the brain is largely due to MAO-B activity (Youdim *et al.*, 2006). Previous studies showed that patients suffering from neurodegenerative diseases, such as AD and PD, have increased activities of MAO-B in the brain and blood platelets (Adolfsson *et al.*, 1980; Alexopoulos *et al.*, 1987).

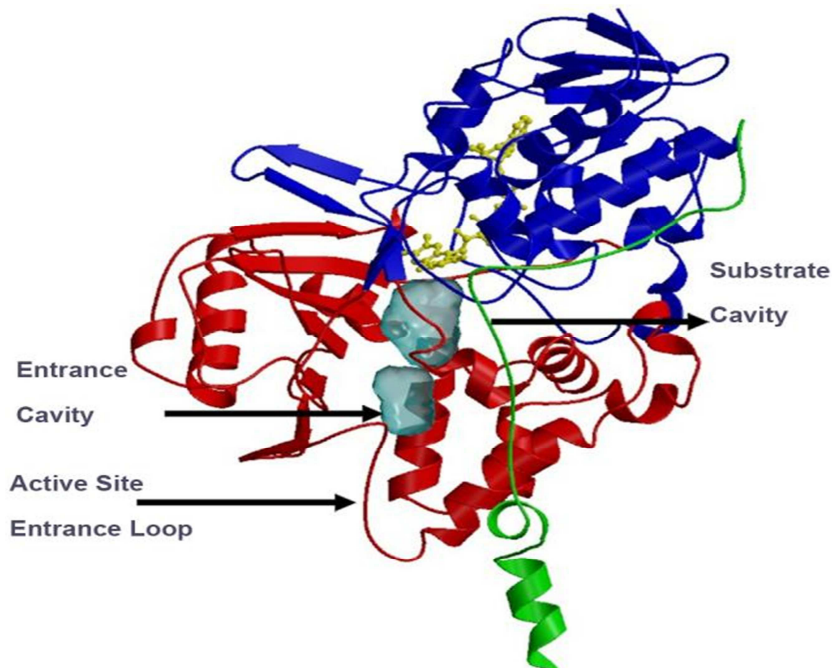
As shown in figure 2.4, DA undergoes oxidative deamination via MAO-B. During its catalytic activity, hydrogen peroxide is produced (Riederer *et al.*, 2004a), as well as the corresponding aldehyde. Either ammonia (in the case of primary amines) or a substituted amine (from secondary amines) is also formed (Youdim *et al.*, 2006). With an increase in age, the expression levels of MAO-B in neuronal tissue increases up to four-fold, resulting in increased levels of DA metabolism and the production of higher levels of hydrogen peroxide and the DA derived aldehyde, dopaldehyde. Because of the increased production of hydrogen peroxide and dopaldehyde, increased MAO-B activity is thought to play a role in the aetiology of neurodegenerative diseases such as PD and AD (Fowler *et al.*, 2003; Kumar *et al.*, 2003).



**Figure 2.4.** The oxidative deamination of DA via MAO-B with the formation of free radicals.

### 2.2.3 The three-dimensional structure of MAO-B

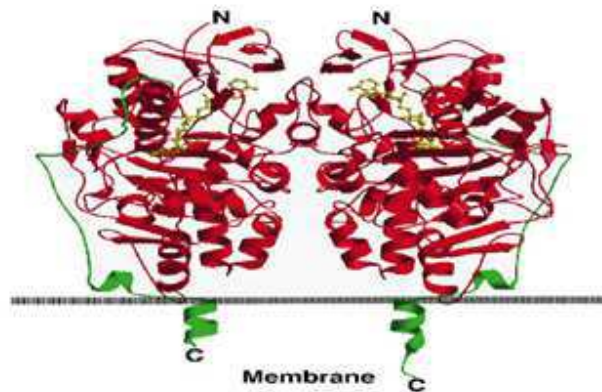
MAO-B, in complex with several pharmacologically important inhibitors, has been solved to a 1.6 Å resolution (Hubálek *et al.*, 2005). Figure 2.5 shows that the active site of the enzyme consists of two cavities, namely a 420 Å hydrophobic substrate cavity and a 290 Å entrance cavity.



**Figure 2.5.** Ribbon diagram of MAO-B showing the entrance cavity and substrate cavity (Edmondson *et al.*, 2007).

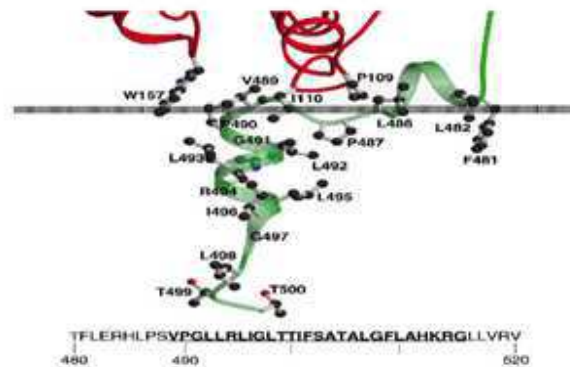
The substrate cavity is lined by a number of aromatic and aliphatic amino acids (Hubálek *et al.*, 2005). The hydrophobic entrance cavity, which is smaller than its adjacent substrate cavity, is lined by residues, Phe 103, Pro 104, Trp 119, Leu 164, Leu 167, Phe 168, Leu 171, Ile 199, Ile 316 and Tyr 326, and is situated between the active site and the protein surface. This smaller entrance cavity is shielded from the solvent by loop 99–112. The two cavities are separated by the side chains of residues, Tyr 326, Ile 199, Leu 171 and Phe 168 (Binda *et al.*, 2002b).

As mentioned earlier, MAO-B is bound to the outer mitochondrial membrane (Edmondson *et al.*, 2004), via the C-terminal segment of the enzyme. The C-terminal segment amino acids involved are residues 461–520. The crystal structure of MAO-B also revealed that it forms dimers on the mitochondrial surface through monomer-monomer interactions as can be seen in figure 2.6 (Binda *et al.*, 2002b).



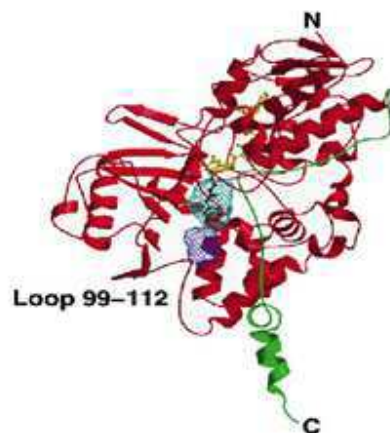
**Figure 2.6.** Ribbon diagram of the MAO-B dimer (Binda *et al.*, 2002b).

Figure 2.7 shows that, in addition to the C-terminus helical segment, other protein regions may also be involved in membrane binding. In the elongated polypeptide stretch, preceding the C-terminus helix of amino acids 481–488, several hydrophobic side chains (Phe 481, Leu 482, Leu 486 and Pro 487) are located close to, and interact with the mitochondrial membrane (Binda *et al.*, 2002b).



**Figure 2.7.** Membrane binding region of one monomer of MAO-B (Binda *et al.*, 2002b).

Also, Pro 109 and Ile 110 at the end of loop 99–112 are surface exposed in such a position that could allow interaction with the membrane. Thus, the presence of these exposed amino acid side chains suggests that membrane attachment does not solely involve the C-terminus helix (Binda *et al.*, 2002b).



**Figure 2.8.** Ribbon diagram of MAO-B indicating loop 99–112 which may regulate entrance to the active site (Binda *et al.*, 2002b).

Admission of a substrate into the active site involves the movement of loop 99–112 to open access to the entrance cavity (figure 2.8). Diffusion of the substrate into the active site begins when a transient movement of the four residues, separating the entrance from the substrate cavities, occurs (Binda *et al.*, 2002b). Figure 2.9 shows the inactivator, rasagiline, attached to the FAD co-factor of MAO-B. The total distance of the substrate migration from the surface of the entrance cavity to the flavin ring is approximately 20 Å (Binda *et al.*, 2002b).

These findings, related to the high resolution crystal structures of human MAO-B, have provided much needed structural information that provides a molecular rationale for further design of novel inhibitors of MAO-B (Hubálek *et al.*, 2005).

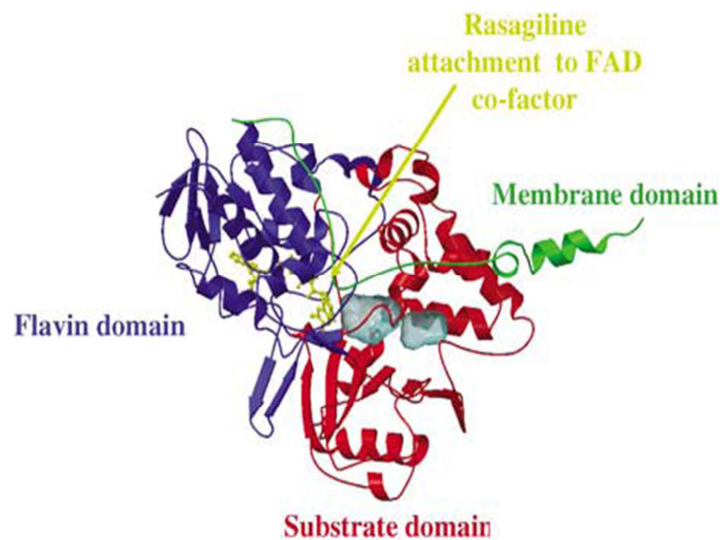


**Figure 2.9.** Ribbon diagram indicating the binding of rasagiline (shown in yellow) to MAO-B (Youdim & Bakhle, 2006).

#### 2.2.4 The three-dimensional structure of MAO-A

As mentioned earlier, MAO-A and MAO-B have a 70% sequence identity (Kearney *et al.*, 1971). The structure of MAO-A has been solved at a resolution of 3 Å and a unique structural feature of MAO-A is that it crystallizes as a monomer (figure 2.10), in comparison with MAO-B, which is a dimer (De Colibus *et al.*, 2005).

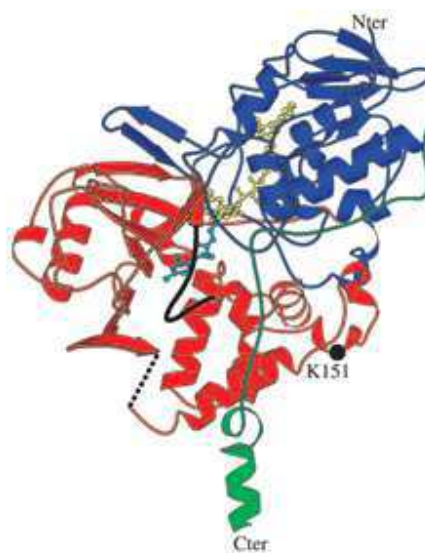


**Figure 2.10.** Ribbon diagram of the MAO-A monomer (De Colibus *et al.*, 2005).

MAO-A differs from MAO-B in that it only possesses a substrate cavity (550 Å), thus lacking an entrance cavity (figure 2.11) (Edmondson *et al.*, 2007).

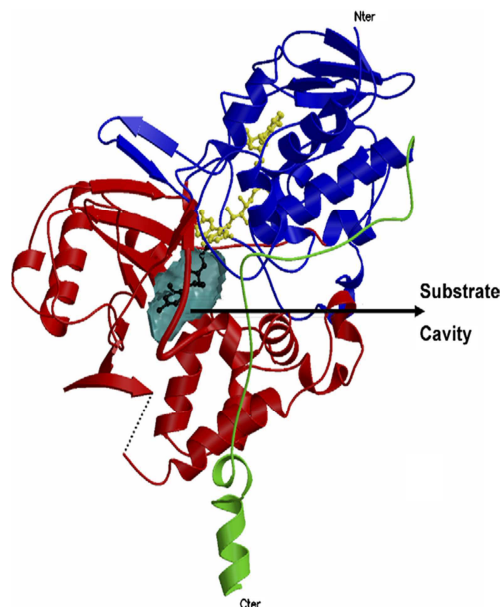


**Figure 2.11.** Ribbon diagram showing MAO-A with its single substrate cavity (Edmondson *et al.*, 2007).

The substrate cavity of MAO-A exhibits a “rounder” shape and is larger in volume than that of MAO-B. The substrate thus has more freedom for rotation in the MAO-A active site than in the MAO-B active site (Edmondson *et al.*, 2007). The reason for the differences in the cavities can be partially attributed to the conformational difference of a six residue segment, namely residues 200–215, that is termed a “cavity shaping loop”. The loop is in a more compact conformation in MAO-B and in a more extended conformation in MAO-A (De Colibus *et al.*, 2005).

### 2.2.5 Catalytic cycle of MAO-B

As mentioned in section 2.2.1, MAO-B is a flavoprotein that catalyzes the oxidative deamination of amines and neurotransmitters. MAO-B contains a covalently bound FAD co-factor as its only redox co-factor, which is absolutely necessary for catalysis (Edmondson *et al.*, 2004).

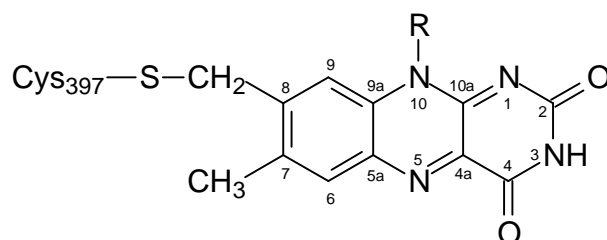


**Figure 2.12.** Chemical structure of the FAD co-factor.

During catalysis, the FAD co-factor is reduced while the amines are oxidized to form an imine product. This is done via an oxidative cleavage of the  $\alpha$ -CH bond of the substrate, a process catalyzed by flavin amine oxidases. The imine product (from primary amine substrates) is then hydrolyzed to an aldehyde and ammonia or to an amine (from secondary and tertiary amine substrates). To complete the cycle, the FAD co-factor is once again oxidized by reaction with oxygen to yield the oxidized form of the FAD, which can be used in another redox reaction (Binda *et al.*, 2002a). A general catalysis reaction is shown in figure 2.13. Before catalysis takes place, a distance of  $\sim 20$  Å must be travelled by the substrate from the entry point to the flavin (Edmondson *et al.*, 2004). Studies have shown that the amine must be deprotonated before binding and catalysis can occur (McEwen *et al.*, 1969).

- $\text{R-CH}_2\text{-NH-R} + \text{FAD}_{\text{OX}} \longrightarrow \text{R-CH=NH}^+\text{-R} + \text{FAD}_{\text{RED}}$
- $\text{R-CH=NH}^+\text{-R} + \text{H}_2\text{O} \longrightarrow \text{R-CH=O} + \text{R-NH}_3^+$
- $\text{FAD}_{\text{RED}} + \text{O}_2 \longrightarrow \text{FAD}_{\text{OX}} + \text{H}_2\text{O}_2$

**Figure 2.13.** General reactions during MAO-B catalysis.

Two mechanisms have been suggested for the electron transfer from the amine to the flavin in MAO catalysis. The first of these is the single electron transfer (SET) mechanism proposed by Silverman (1995). Figure 2.14 illustrates the SET mechanism.

Firstly, a one-electron transfer takes place from the lone pair on the amine nitrogen to the FAD, to yield an aminium cation radical and a flavin radical. Secondly, an  $\text{H}^+$  from the  $\alpha$ -carbon is abstracted by an active site base in the catalytic site. Unfortunately structural data on MAO-B shows no amino acid residues that could perform this role. In the last step, the second electron is transferred from the amine substrate to the FAD to yield the two-electron oxidized product, the corresponding imine. When considering the energetics of the oxidized flavin acting as a one

electron oxidant of the amine, the conclusion can be made that the SET mechanism for amine oxidation is both kinetically and thermodynamically improbable (Edmondson *et al.*, 2004).

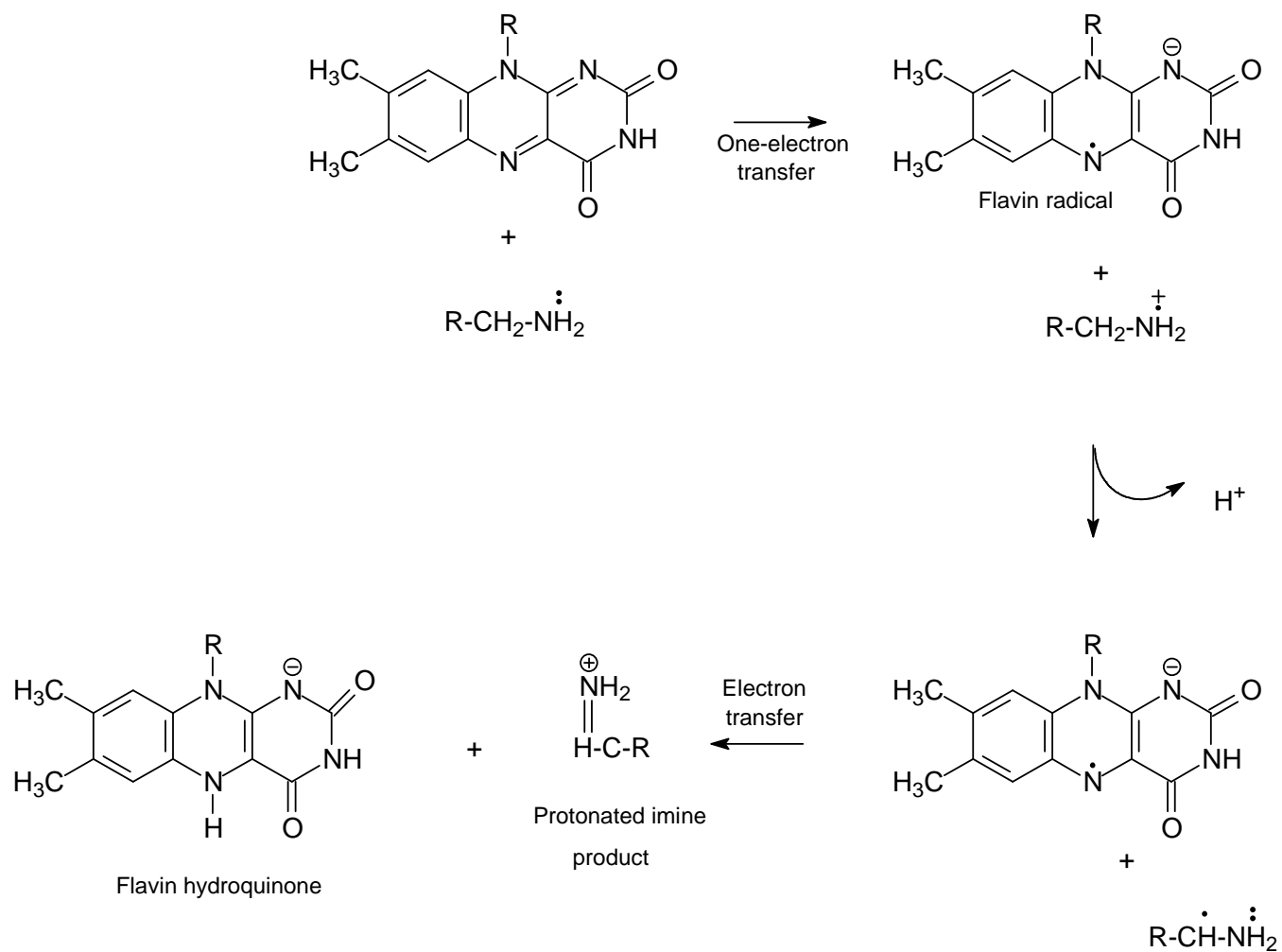


**Figure 2.14.** The SET mechanism of MAO catalysis.

The second mechanism that has been proposed for MAO catalysis is depicted in figure 2.15. This mechanism is the polar nucleophilic mechanism.

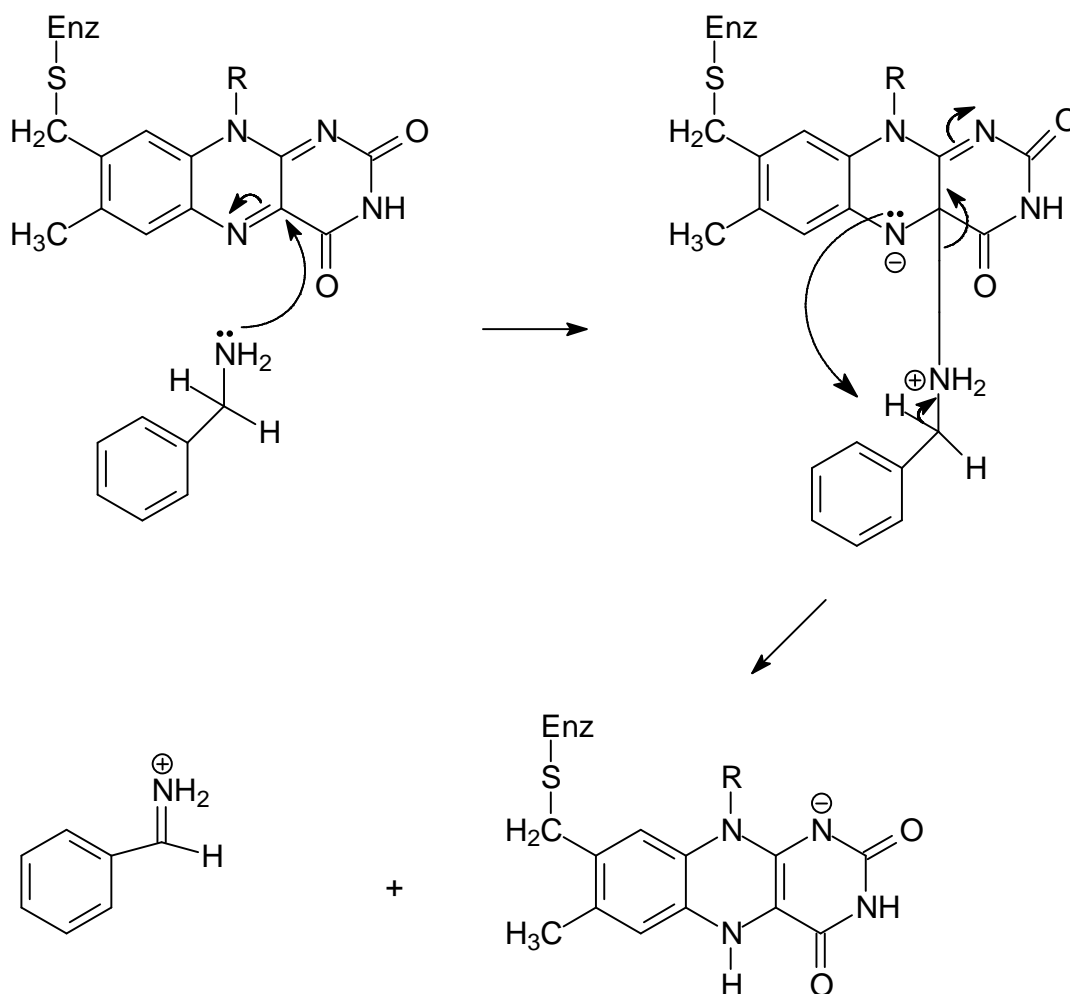


**Figure 2.15.** The polar nucleophilic mechanism of MAO catalysis.

Firstly, the deprotonated amine launches a nucleophilic attack on the C(4a) position of the flavin, after which the N(5) position of the flavin becomes a strong enough base to abstract a H<sup>+</sup> from the substrate. The H<sup>+</sup> which is being abstracted is almost always in the R-configuration and is termed  $\alpha$ -pro-R-H (Edmondson *et al.*, 2004). According to evidence from Edmondson *et al.* (2004), the MAO-B catalysis proceeds via a polar nucleophilic mechanism, rather than a SET mechanism.

### 2.2.6 Clinically used inhibitors of MAO-B

MAO-inhibitors can be classified into three types, namely (1) irreversible, nonselective agents such as tranylcypromine, (2) irreversible, selective MAO-B agents such as selegiline and rasagiline and (3) reversible, selective MAO-B agents such as lazabemide (Riederer *et al.*, 2004b).

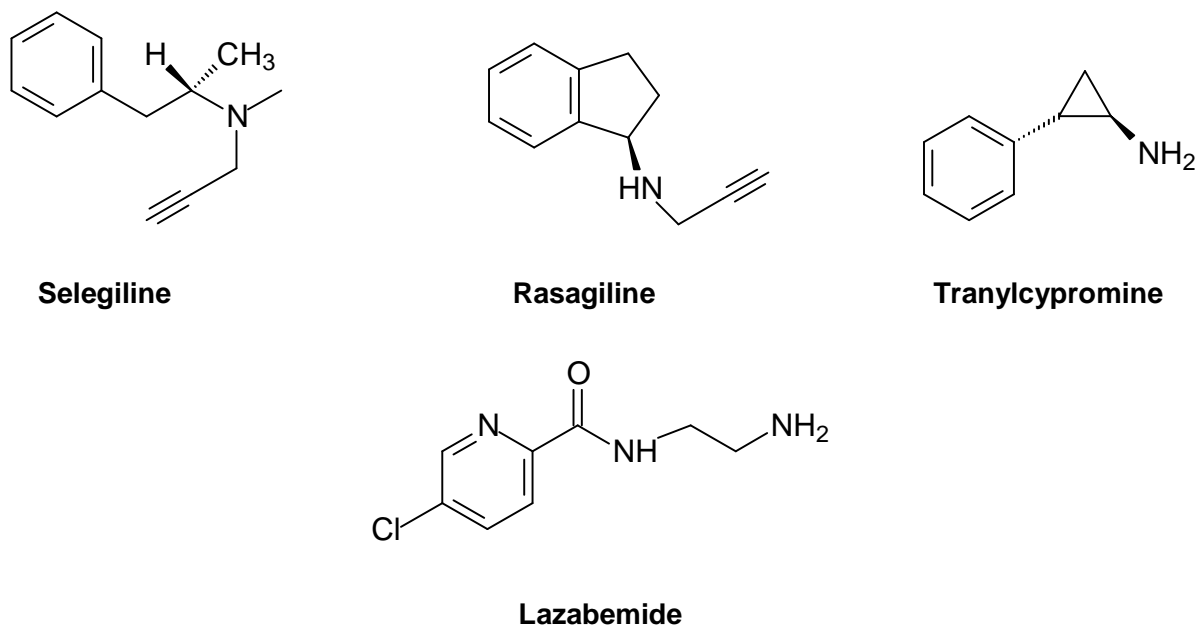


**Figure 2.16.** Chemical structures of selegiline, rasagiline, tranylcypromine and lazabemide.

Tranylcypromine, an irreversible nonselective inhibitor of both the isoforms of MAO, may lead to the formation of the so called “cheese reaction” (Youdim *et al.*, 1988). As mentioned earlier, MAO-A metabolizes NA, adrenaline, tyramine, DA and 5-HT (Johnston, 1968) whereas MAO-B metabolizes only DA and tyramine (Youdim *et al.*, 2005). The “cheese reaction” occurs when MAO-A in the gastrointestinal tract is inhibited (as can be seen with tranylcypromine) and exogenous sources of tyramine are ingested such as beer, wine and certain cheeses. The result is increased blood tyramine levels. Tyramine is a NA releaser in the brain and, since MAO-A is inhibited, an excess of tyramine enters the systemic circulation, which leads to an excessive amount of NA released and a severe hypertensive response may occur (Finberg *et al.*, 1981; Finberg & Tenne, 1982). Thus, the development of specific, reversible MAO-B inhibitors that are safer, could lead to clinically useful neuroprotective agents (Hubálek *et al.*, 2005).

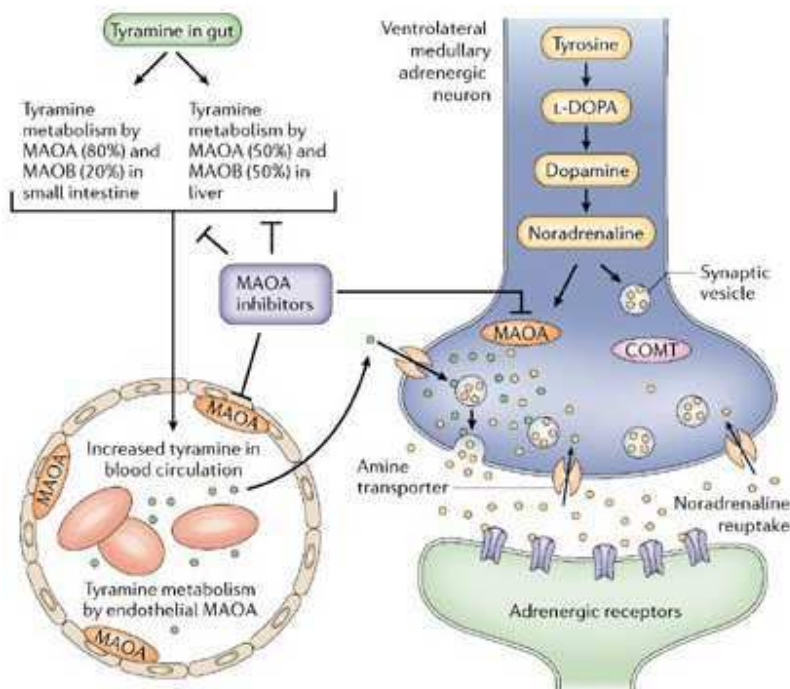


**Figure 2.17.** Schematic representation of the “cheese reaction” (Youdim & Bakhle, 2006).

Previous studies have shown that selegiline can be clinically used as an antiparkinsonian agent and that this drug is neuroprotective in 1-methyl-4-phenyl-1,2,3,6-tetrahydropyridine (MPTP) treated animals (Heikkila *et al.*, 1984b). Moreover, it may also reduce oxidative stress, protect from apoptotic processes, reduce L-Dopa doses required for the treatment of PD and may improve DA's profile to continuous stimulation of DA receptors (Riederer *et al.*, 2004b). A preliminary analysis showed that patients receiving selegiline in combination with L-Dopa had a better survival rate than those treated with L-Dopa alone (Birkmayer *et al.*, 1985).

Selegiline exhibits at least seven accepted mechanisms by which it could prevent neurodegeneration (Gerlach *et al.*, 1996):

1. The inhibition of MAO-B may decrease the formation of free radicals (hydrogen peroxide) when DA is metabolized (Cohen & Spina, 1989).
2. It may elevate superoxide dismutase activity to increase the free radical scavenging capacity in the brain (Carrillo *et al.*, 1991; Knoll, 1988).
3. Inhibition of MAO-B may prevent activation of environmental pre-toxins (Langston, 1990).

4. Oral administration may inhibit the oxidation of low-density lipoprotein (LDL) (Thomas *et al.*, 2002) which suggests that, with long term use, it may be anti-atherogenic and cardioprotective.
5. It was shown to reduce the secretion of neurotoxic products by stimulated human monocytic THP-1 cells (Klegeris & McGeer, 2000).
6. It exhibits protective effects against neuronal apoptosis in cell culture (Suuronen *et al.*, 2000).
7. It may attenuate neuronal damage due to the uptake inhibitory properties at nerve endings (Magyar, 1994).

Selegiline, unfortunately, undergoes extensive first-pass hepatic metabolism and has a relatively low absolute bioavailability (~10%) (Mahmood *et al.*, 1995; Mahmood, 1997). Thus 90% is metabolized before it reaches the systemic circulation (Mahmood, 1997; Haberle *et al.*, 2002). The metabolites formed, namely desmethylselegiline, L-methamphetamine and L-amphetamine are potentially neurotoxic and may possibly be associated with adverse cardiovascular and psychiatric effects (Montastruc *et al.*, 2000; Churchyard *et al.*, 1999; Gill *et al.*, 1967; Churchyard *et al.*, 1997). Moreover, in higher doses it loses selectivity for MAO-B which may potentially lead to the dangerous “cheese reaction” when MAO-A is also inhibited. As such, these neurotoxic effects may neutralize its neuroprotective effects and may also compromise its safety in patient populations (Oh *et al.*, 1994; Abu Raya *et al.*, 2002; Bar Am *et al.*, 2004).

Rasagiline on the other hand, is also an irreversible selective MAO-B inhibitor but after first pass hepatic metabolism, it does not form amphetamine metabolites, but rather an inactive metabolite known as aminoindan (Chen & Swope, 2005). It has an approximate bioavailability of 36% (Chen & Swope, 2005) and is 3–15 times more potent than selegiline (Youdim *et al.*, 2001). At higher doses, it also loses some of its specificity for MAO-B (Youdim *et al.*, 2001), however, clinical data shows no evidence of the potential for the occurrence of the “cheese reaction” (deMarcaida *et al.*, 2006).

Certain studies have shown that people who never smoked are twice as likely to develop PD than smokers (Allam *et al.*, 2004; Hernán *et al.*, 2001), and people ingesting no or very low quantities of caffeine are also at risk in developing PD (Ascherio *et al.*, 2004; Ascherio *et al.*, 2003). This led to the conclusion that drugs containing caffeine and components of tobacco smoke may be developed as neuroprotective drugs for the treatment of PD. (E)-8-(3-

Chlorostyryl)caffeine (CSC), which is an A<sub>2A</sub> receptor antagonist and trans,trans-farnesol, which is a component of tobacco smoke, were found to be potent, reversible inhibitors of MAO-B (Fowler *et al.*, 2003). CSC, which also antagonizes the A<sub>2A</sub> receptor in addition to inhibiting MAO-B, may represent a novel means of treating PD.

### **2.2.7 Genetics**

Through cDNA cloning, the amino acid sequences of both the MAO isoforms were elucidated (Nagatsu, 2004). This showed that they share a 70% sequence identity, with MAO-A consisting of 527 amino acids with a molecular weight of 59700 and MAO-B consisting of 520 amino acids with a molecular weight of 58000. Both isoforms contain the pentapeptide Ser-Gly-Gly-Cys-Tyr and the FAD cofactor is covalently bound via a thio ether linkage to the cysteine (Bach *et al.*, 1988; Chen *et al.*, 1991). The FAD in MAO-B is covalently linked to Cys397 and to Cys406 in MAO-A (Abell & Kwan, 2001).

The MAO genes are situated on the X chromosome of humans and both genes are closely located between bands Xp11.23 and Xp22.1 (Lan *et al.*, 1989). Both isoforms' genes consist of 15 exons and have identical exon-intron organization. The most conserved exon, namely exon 12, encodes for the covalent FAD-binding site and shows 93.9% amino acid identity between MAO-A and MAO-B. This suggests that the two isoforms share a common ancestral gene (Grimsby *et al.*, 1991). In rare cases, the genes encoding for the MAOs are deleted, leading to Norrie's disease which is characterized by blindness, hearing loss and mental retardation (Lan *et al.*, 1989).

## **2.3 MPTP**

### **2.3.1 General background**

In the 1980s, young drug users presented to several emergency rooms after developing symptoms very similar to that of PD (Burns *et al.*, 1985; Langston, 1985). This was traced back to the intravenous use of a street preparation of 1-methyl-4-phenyl-4-propionpiperidine (MPPP), an analogue of the narcotic meperidine (Langston *et al.*, 1983). MPTP, a proneurotoxin, was the responsible neurotoxic contaminant, produced during the synthesis of MPPP. After the neurotoxic effects were discovered in humans, only then were animal models developed (Smeyne & Jackson-Lewis, 2004). The mechanism by which MPTP selectively damages nigrostriatal neurons and induces a parkinsonian syndrome has been the subject of extensive research (Heikkila *et al.*, 1984a; Nicklas *et al.*, 1985; Smeyne & Jackson-Lewis, 2004).

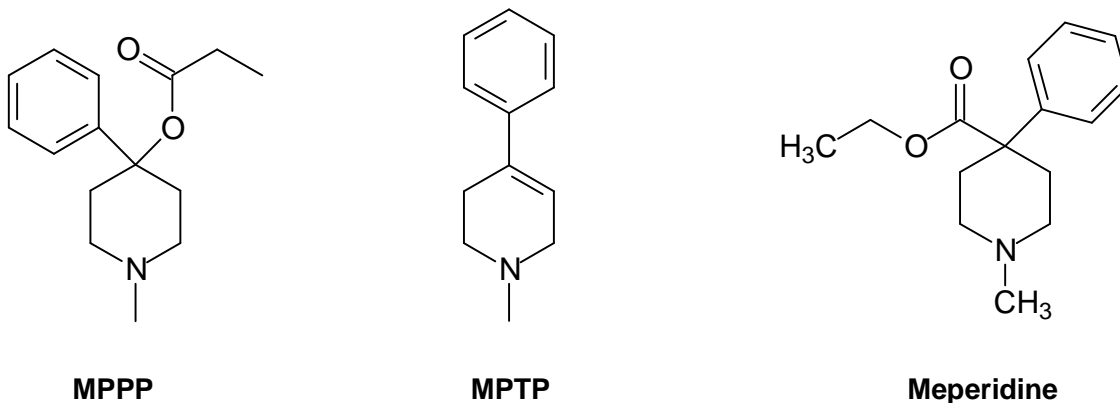


**Figure 2.18.** Chemical structures of MPPP, MPTP and meperidine.

### 2.3.2 Mechanism of MPTP action

MPTP, after systemic administration, crosses the BBB because of its highly lipophilic nature. Once in the brain, more specifically in the glial cells, the pro-neurotoxin is oxidized by MAO-B to MPDP<sup>+</sup> (Dauer & Przedborski, 2003). MPDP<sup>+</sup> once again undergoes a second two-electron oxidation, via an unknown mechanism, to generate the ultimate neurotoxin, MPP<sup>+</sup> as can be seen in figure 2.19 (Chiba *et al.*, 1984; Ramsay *et al.*, 1991; Markey *et al.*, 1984).

MPP<sup>+</sup> then moves out of the glial cells into the extracellular space via an unknown mechanism. MPP<sup>+</sup> is taken up into the dopaminergic cells by the dopamine transporter (DAT), and once in the cell, it can move through several cellular compartments such as the mitochondria (Smeyne & Jackson-Lewis, 2004). MPP<sup>+</sup> accumulates in the inner mitochondrial membrane, a process which is driven by an electrical gradient (Ramsay & Singer, 1986; Ramsay *et al.*, 1986). Degeneration of nigrostriatal dopaminergic neurons occurs when MPP<sup>+</sup> inhibits complex I of the mitochondrial respiratory chain, an event which leads to ATP depletion and oxidative stress, as can be seen in figure 2.20 (Singer *et al.*, 1988). The subsequent depletion of striatal DA is indicative of the permanent loss of nigrostriatal dopaminergic cell bodies in the substantia nigra.

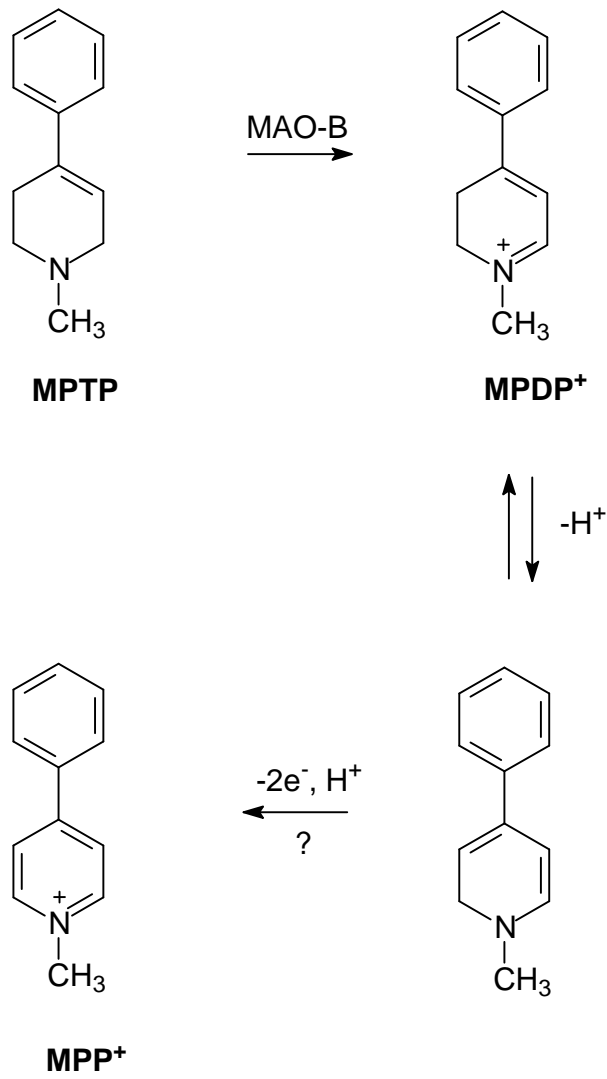


**Figure 2.19.** The MAO-B catalyzed oxidation of MPTP to the intermediate MPDP<sup>+</sup> and MPP<sup>+</sup>.

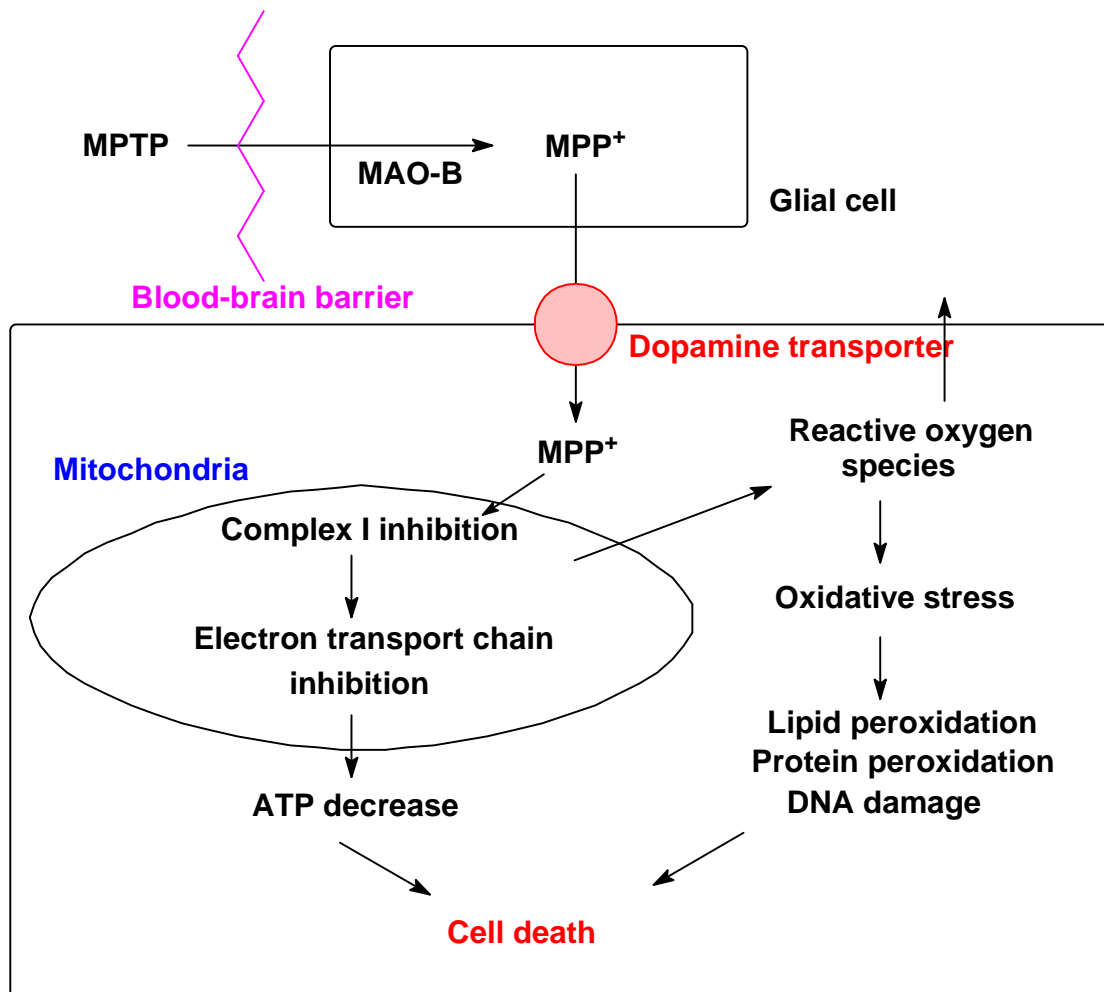


**Figure 2.20.** Schematic representation depicting the mechanism of action of MPTP in the nigrostriatal system.

## 2.4 Enzyme kinetics

### 2.4.1 Introduction

Enzyme kinetics can be defined as the field of biochemistry which is concerned with the quantitative measurement of the rates of enzyme-catalyzed reactions and the study of the factors that influence these rates. Some of these factors include temperature, substrate concentrations and activation energies. It is also used to determine the inhibitory potencies of certain agents which reduce the rates of specific enzyme-catalyzed processes.

## 2.4.2 The Michaelis-Menten equation

The Michaelis-Menten equation illustrates the relationship between the initial reaction velocity ( $V_i$ ) and the substrate concentration ( $[S]$ ):

$$V_i = \frac{V_{max}[S]}{K_m + [S]}$$

$V_i$  can be defined as the rate of the forward reaction, the combination of a substrate with an enzyme (E) to form a product. Enzyme activity assays are almost always conducted when there is an excess substrate over enzyme, and when this occurs,  $V_i$  will be directly proportionate to the enzyme concentration ( $V_i \propto [E]$ ). As the substrate concentration is increased,  $V_i$  will also be increased until it reaches a maximum value that is termed  $V_{max}$ . When further increases in substrate concentration do not increase  $V_i$ , then the enzyme is said to be saturated (Murray *et al.*, 2003).

$K_m$  in the Michaelis-Menten equation is termed the Michaelis-Menten constant and is the substrate concentration where  $V_i$  equals half of  $V_{max}$ :

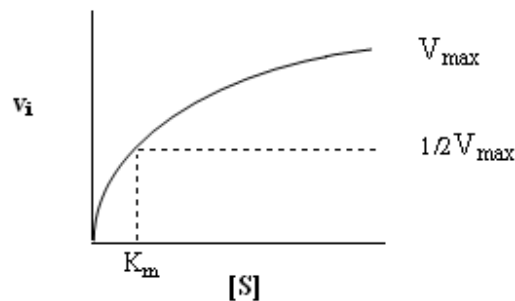


**Figure 2.21.** Effect of the substrate concentration on the initial velocity of an enzyme-catalyzed reaction.

The Michaelis-Menten equation can be evaluated under three conditions (Murray *et al.*, 2003):

1. When  $[S]$  is much less than  $K_m$ , then the term  $K_m + [S]$  can be set equal to  $K_m$ . The Michaelis-Menten equation is then reduced to:

$$V_i = \frac{V_{max}[S]}{K_m + [S]}$$

2. When [S] is much greater than  $K_m$ , then the term  $K_m + [S]$  can be set equal to [S]. The Michaelis-Menten equation is then reduced to:

$$V_i = V_{max}$$

Thus the initial velocity is at the maximal rate.

3. When [S] equals  $K_m$ , then the Michaelis-Menten equation can be reduced to:

$$V_i = \frac{V_{max}}{2}$$

Thus the initial velocity is at half-maximal rate.

In order to determine numeric values of  $V_{max}$  and  $K_m$ , impractically high concentrations of substrate is needed to achieve saturation. But rearranging the Michaelis-Menten equation into an equation for a straight line, circumvents this problem and  $V_{max}$  and  $K_m$  can be calculated at very low concentrations of the substrate:

$$\frac{1}{V_i} = \frac{K_m}{V_{max}} \cdot \frac{1}{[S]} + \frac{1}{V_{max}}$$

The equation above can now be used to construct a straight-line which is termed a double reciprocal or Lineweaver-Burk plot. By setting y equal to zero, and solving for x, the  $K_m$  value may be determined, since the x-intercept is equal to  $-1/K_m$ :

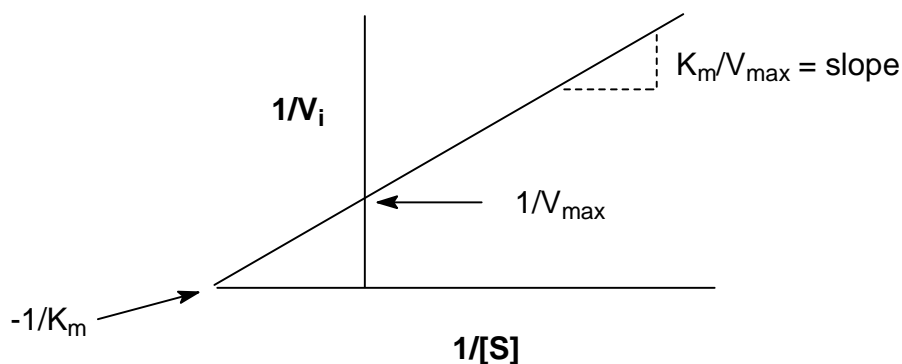


**Figure 2.22.** The Lineweaver-Burk plot.

Lineweaver-Burk plots can be used to distinguish between competitive and non-competitive inhibition. As mentioned earlier, enzyme kinetics are used to determine the inhibitory potency of certain agents, and this inhibitor potency is expressed by the inhibitor constant,  $K_i$ .  $V_i$  can be calculated both in the presence or absence of certain inhibitors at several substrate concentrations. Once plotted, it can be seen that, when two lines are plotted for competitive inhibition, one in the presence of an inhibitor and the other in the absence of an inhibitor, both lines have a common intercept on the y-axis:

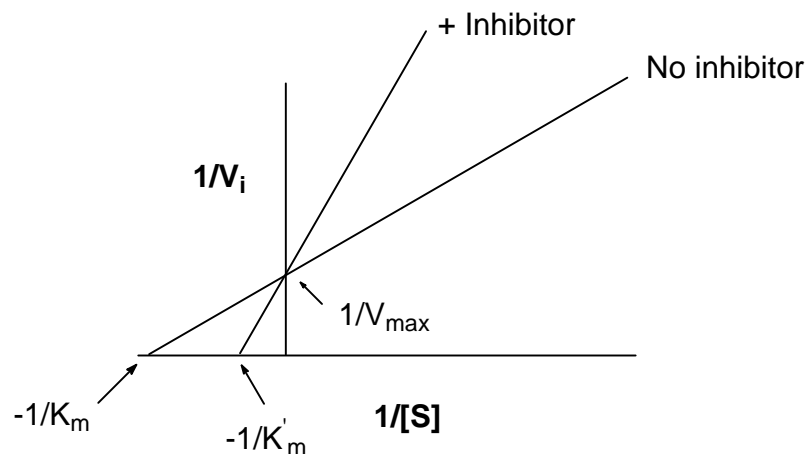


**Figure 2.23.** Lineweaver-Burk plot during competitive inhibition.

Thus, a competitive inhibitor has no effect on  $V_{max}$ , but raises  $K'_m$ , the apparent  $K_m$  for the substrate.  $K_i$  can now be calculated from the following equation, once  $K_m$  has been determined in the absence of an inhibitor:

$$x = \frac{-1}{K_m} \left( 1 + \frac{[I]}{K_i} \right)$$

$K_i$  values can be used to determine inhibitory properties of agents to the same enzyme. The lower the value of  $K_i$ , the more potent the inhibitor will be and *vice versa*.

In non-competitive inhibition, the binding of the inhibitor does not affect the binding of the substrate. Non-competitive inhibitors thus lower the value of  $V_{max}$  but have no effect on  $K_m$  (Murray *et al.*, 2003):

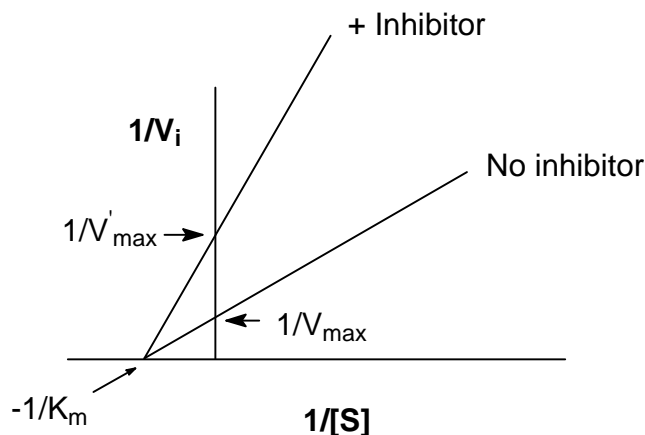


**Figure 2.24.** Lineweaver-Burk plot during non-competitive inhibition.

### 2.4.3 IC<sub>50</sub> value calculation

IC<sub>50</sub> values are defined as the concentration of the inhibitor that produces 50% inhibition. IC<sub>50</sub> values are another way to express inhibitor potency. The relationship between the IC<sub>50</sub> value and the K<sub>i</sub> can be seen from the following (Cheng and Prusoff, 1973):

$$K_i = IC_{50} / (1 + [S]/K_m)$$

In this study, the MAO inhibition potencies of the test inhibitors will be expressed as the IC<sub>50</sub> values. To experimentally determine IC<sub>50</sub> values, the initial enzyme catalytic rates are measured in the absence and presence of various concentrations of the inhibitor. The catalytic rates are subsequently plotted versus the logarithm of the inhibitor concentration to obtain a sigmoidal curve. The concentration of the inhibitor that reduces the rate recorded in the absence of inhibitor by 50% is equal to the IC<sub>50</sub> value of the inhibitor. An example of a rate-concentration sigmoidal curve will be presented in chapter 4.

## 2.5 Conclusion

This chapter described PD as being a progressive neurodegenerative disorder. It was shown that the MAO-B enzyme plays an important role in PD since MAO-B metabolizes DA. Inhibitors of MAO-B are therefore useful agents for the treatment of PD, since such drugs may conserve DA in the parkinsonian brain. In addition, MAO-B inhibitors may also reduce the formation of potentially neurotoxic metabolic by-product of MAO catalysis in the brain. The following chapter describes the synthesis of caffeine derived structures, which may act as inhibitors of MAO-B.